Steel and Composite Structures, *Vol. 18, No. 1 (2015) 71-90*
DOI: http://dx.doi.org/10.12989/scs.2015.18.1.071

Axial behaviour of rectangular concrete-filled cold-formed steel tubular columns with different loading methods

Xiushu Qu [1,2], Zhihua Chen [*2] and Guojun Sun [2]

[1] *School of Civil and Transportation Engineering, Beijing University of Civil Engineering and Architecture, Beijing, 100044, P.R. China*
[2] *School of Civil Engineering, Tianjin University, Tianjin, 300072, P.R. China*

(*Received December 14, 2012, Revised December 10, 2013, Accepted May 21, 2014*)

Abstract. Axial compression tests have been carried out on 18 rectangular concrete-filled cold-formed steel tubular (CFST) columns with the aim of investigating the axial behaviour of rectangular CFST columns under different loading methods (steel loaded-first and full-section loaded methods). The influence of different loading methods on the ultimate strength of the specimens was compared and the development of Poisson's Ratio as it responds to an increasing load was reported and analysed. Then, the relationship between the constraining factor and the strength index, and the relationship between the constraining factor and ductility index of the specimens, were both discussed. Furthermore, the test results of the full-section loaded specimens were compared with five international code predicted values, and an equation was derived to predict the axial carrying capacity for rectangular CFST columns with a steel loaded-first loading method.

Keywords: axial carrying capacity; constraining factor; ductility index; loading method; poisson's ratio; rectangular concrete-filled cold-formed steel tubular; strength index

1. Introduction

Concrete-filled steel tubular (CFST) columns are gaining increasing usage in modern construction practice with many advantages in terms of higher load carrying capacity, larger energy absorption and better ductility performance. The developments in pumping techniques and high strength concrete in the 1980s drove a rapid increase in the use of CFST columns within the construction of high-rise buildings, long span bridges and heavy industrial buildings (Yang *et al*. 2008). The outer skins of existing CFST sections mainly represented with square, rectangular or circular profiles. Circular tubular columns have an advantage over all other sections when used in compression members for a given cross-sectional area; and they have a large uniform flexural stiffness in all directions. Rectangular hollow sections (*RHSs*) have the structural advantages of rectangular sections with different major and minor axis properties; which enable members to be orientated so as to most effectively resist the applied loading. Furthermore, on account of the geometrical characteristic, the making of the beam-column connection of rectangular CFST column- H beam is much easier than that of a circular CFST column –H beam.

*Corresponding author, Professor, E-mail: zhchen@tju.edu.cn

http://www.techno-press.org/?journal=scs&subpage=8 ISSN: 1229-9367 (Print), 1598-6233 (Online)

In the past, many studies had been conducted with respect to rectangular CFST columns to investigate the static and dynamic behaviours of the columns which made use of certain methods of experimental study and numerical models. A review of relevant developments in the area of research of rectangular CFST columns in construction before 2000 has been carried out by Han (Han 2002). From Han's research onwards, the research on rectangular CFST columns has been further continued. This subsequent research is focused on the following points: the usage of high strength material and stiffeners to increase the overall strength, the building of rectangular CFST columns numerical models and the improvement of design expressions. In 2002, Han experimentally studied the performance of rectangular CFST stub columns and analyzed the influence of constraining factors and the width-to-thickness ratio on column behaviour (Han 2002). The constraining factor, as a concept, was first introduced in 2001 to describe the composite action that takes place between the steel tube and filled concrete (Han 2001), the constraining factor is defined as $\xi = A_s f_{sy} / A_c f_{ck}$ (1). Since research work related to rectangular sections with higher concrete strength is still at a limited stage this, therefore, deserves yet further investigation. Lue *et al*. (2007) tested 24 rectangular CFST columns to investigate the behaviour of rectangular CFST columns with high strength concrete subjected to axial loading. On account of there being a distinct lack of design code available that can be used specifically on the design of stiffened thin-walled composite columns, it was considered necessary by Tao *et al*. (2009) to discuss the limit of the width-to-thickness ratio for the sub-panels and the rigidity of requirement for the stiffeners. Based on further test results, Muhammad proposed an equation to estimate the ultimate axial compressive loading capacities for square CFST columns (Muhammad *et al*. 2006). Next, Giakoumelis and Lam (2004) proposed a coefficient for the ACI/AS equation to take into account the effect of concrete confinement on the axial load capacity of concrete confinement on the axial load capacity. Following this, Yang proposed simplified formulae to predict the ultimate strength of CFST stub columns loaded on the partial cross-sectional area (Yang and Han 2009). Based on the nonlinear behaviour of concrete-filled high strength stainless steel stiffened slender square and rectangular hollow section columns, a design equation was subsequently proposed by Ellobody (2007) for concrete-filled stainless steel stiffened slender tube columns.

Besides, some other researchers have down many research on the axial carrying capacity, the main parameters affecting the carrying capacity are the *D*/*t* radio (Moon *et al*. 2012, Gupta *et al*. 2007, EI-Heweity 2012, Muhammand *et al*. 2006), materials properties (Moon *et al*. 2012, Song *et al*. 2010, Gupta *et al*. 2007, Yuan and Yang 2013, Tokgoz and Dundar 2010, Liang 2011, Patel *et al*. 2012), fire duration time (Song *et al*. 2010), axial load ratio (Song *et al*. 2010), steel ratio (Song *et al*. 2010, Gupta *et al*. 2007), slenderness radio (Gupta *et al*. 2007, Yuan and Yang 2013, Tokgoz and Dundar 2010, Patel *et al*. 2012, Muhammand *et al*. 2006), hollow section ratio (Yuan and Yang 2013), cross section (Tokgoz and Dundar 2010, Lam 2012, Muhammand *et al*. 2006), eccentricity of loading (Patel *et al*. 2012) and temperature (Lam 2012, Song *et al*. 2010). Almost all previous experimental studies on the behaviour of the rectangular CFST columns have adopted the full section-loaded method (see, Fig. 1(a), Full section loaded method). All the specimens are prepared suitably to make sure the concrete achieves the same height as the steel tube within the test process. Two steel blocks are usually attached at the two ends to make sure the force is applied equally across the entire cross-section. However, it should be noted that actual loading form is not performed in isolation in practical engineering. For example, before the concrete reaches sufficient strength, there may be some initial stress in the steel tubes due to the gravity of the upper load. This is shown in the Fig. 1(b) namely: pre-stress in the steel tube; and, due to concrete's ability to shrink, the load may only be applied on the steel tube in the first instance, as illustrated in Fig. 1(c),

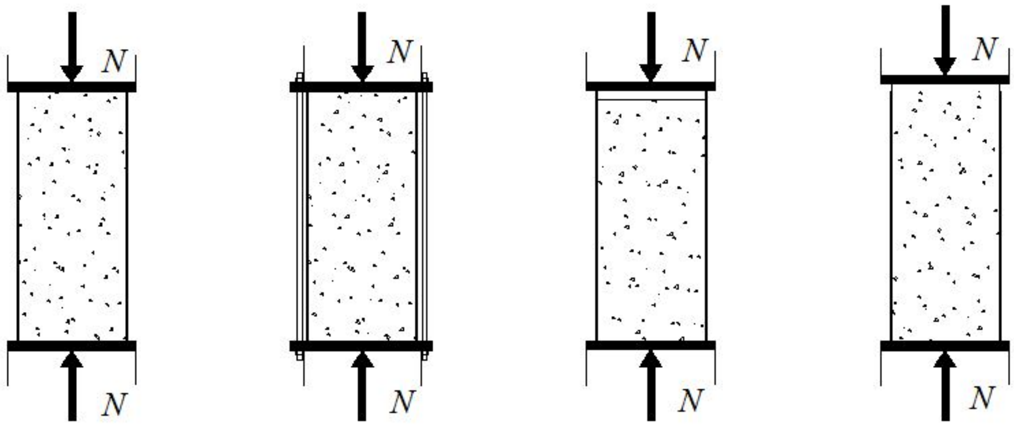

Fig. 1 Different loading methods

by the steel loaded-first method; furthermore, in constraining CFST piers, loading is mainly to be applied on the core-concrete, as shown in Fig. 1(d) with the concrete loaded- first method.

Some experimental research in relation to the behavior of CFST columns undergoing an initial stress has been conducted by Han in 2003 and Xiong in 2007 (Han and Yao 2003, Xiong and Zha 2007). Chen and Huang (2009) found that, when specimens are subjected to a load that acted only on the steel tube at two ends throughout the whole process, the ultimate load carrying capacity and stiffness decreased obviously; and the constraining effect of outer steel on core concrete could be neglected (Chen and Huang 2009). But for the pattern C – steel loaded method, different boundary conditions at the two ends show different influences on the ultimate carrying capacity. Within practical engineering, the method whereby specimens are loaded exclusively onto the steel tube at the topmost end and are restricted across the full section at the bottom end is far more commonly-found. Study on the behavior of rectangular CFST columns steel-loaded at one end only is still deficient and therefore deserves further investigation.

In the present investigation a series of tests on rectangular CFST columns has been performed. The experimental study has focussed on the axial compression behaviour of different loading methods as applied to rectangular CFST columns. In addition the Poisson's Ratio, strength index, ductility index and ultimate carrying capacity comparison of the specimens subjected to different loading have, in each case, been reported and analysed. Based on the measured strain values of the steel tube, the proportion of the total load that has been shared by the steel section has also been discussed. All the test data has been analysed and compared relative to predictions derived from five well-known international structural design codes. Design recommendations have been presented on the basis of the comparisons.

2. Experimental study

2.1 General

A total of 18 rectangular CFST stub columns were tested to investigate axial compression behaviour subjected to different loading methods. The variables investigated were selected as: (a) loading method; (b) cross-section dimension; (c) concrete compressive strength; and (d) steel grade. Table 1 provides details of the ranges of values and loading methods covered within the study. For all the specimens, designations starting with ZYA refer to those that have been loaded onto the steel tube at the topmost end and that cover the full cross-section at the bottom end; while designations starting with ZYB refer to those which were loaded onto the full cross-section at both of the ends. Added to the initial three-letter designation letter code are the specimen numbers: ranging from 1 to 9. The constraining factor (ξ), which is used to capture geometric and material

Table 1 Specimen details for the axial loading tests

Specimen reference	$D \times B \times t \times L$ (mm)	Concrete strength grade	Steel grade	ξ	$N_{u,e}$ (kN)	Loading method
ZYA-1	150 × 100 × 4.065 × 700	C30	Q235b	2.14	950	Steel-loaded
ZYA-2	150 × 100 × 4.065 × 800	C40	Q235b	1.61	1262	Steel-loaded
ZYA-3	150 × 100 × 4.065 × 900	C50	Q235b	1.28	990	Steel-loaded
ZYA-4	200 × 150 × 4.433 × 700	C50	Q235b	0.78	2100	Steel-loaded
ZYA-5	200 × 150 × 4.433 × 800	C30	Q235b	1.31	1660	Steel-loaded
ZYA-6	200 × 150 × 4.433 × 900	C40	Q235b	0.98	2095	Steel-loaded
ZYA-7	300 × 200 × 5.730 × 800	C40	Q345b	1.25	4200	Steel-loaded
ZYA-8	300 × 200 × 5.730 × 900	C50	Q345b	0.99	4500	Steel-loaded
ZYA-9	300 × 200 × 5.730 × 1000	C30	Q345b	1.66	3580	Steel-loaded
ZYB-1	150 × 100 × 4.065 × 700	C30	Q235b	2.14	1000	Full section-loaded
ZYB-2	150 × 100 × 4.065 × 800	C40	Q235b	1.61	1200	Full section -loaded
ZYB-3	150 × 100 × 4.065 × 900	C50	Q235b	1.28	1000	Full section -loaded
ZYB-4	200 × 150 × 4.433 × 700	C50	Q235b	0.78	1380	Full section -loaded
ZYB-5	200 × 150 × 4.433 × 800	C30	Q235b	1.31	1400	Full section -loaded
ZYB-6	200 × 150 × 4.433 × 900	C40	Q235b	0.98	2000	Full section -loaded
ZYB-7	300 × 200 × 5.730 × 800	C40	Q345b	1.25	3600	Full section -loaded
ZYB-8	300 × 200 × 5.730 × 900	C50	Q345b	0.99	3450	Full section -loaded
ZYB-9	300 × 200 × 5.730 × 1000	C30	Q345	1.66	3550	Full section -loaded

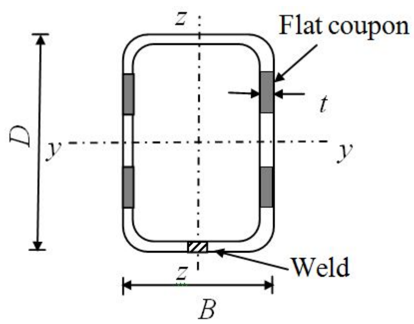

Fig. 2 Section labelling convention

Fig. 3 Specimen with a gap of 10 mm at top

Table 2 Key material properties from tensile coupons tests

Specimen	Young's modulus E_s (*MPa*)	Yield stress f_y (MPa)	Ultimate strength f_u (MPa)
RHS 150 × 100 × 4.065	212300	295	496
RHS 200 × 150 × 4.433	216800	242	410
RHS 300 × 200 × 5.730	216400	336	533

Table 3 Measured concrete properties

Concrete strength grade	Young's modulus E_c (MPa)	Compressive strength f_{cu} (MPa)
C30	26690	31
C40	2938 0	41
C50	38070	52

parameters and categorise them into a single combined parameter, is listed in Table 1. The section's details as to labelling convention are variously shown in Fig. 2.

2.2 Preparation of specimens

Three types of cold-formed rectangular steel tubes with different thicknesses were used in the construction of the specimens. To accomplish the pattern C loading method (steel loaded-first), a kind of wood plate with a thickness of 10 mm was put at the bottom of each Group ZYB tube before the concrete was poured in. After the specimens had been cured for 28 days, the wood plate was taken out as shown in Fig. 3.

The nominal tube thicknesses are 4 mm, 5 mm and 6 mm respectively. The basic stress-strain characteristics of the rectangular steel tubes were obtained by means of tensile coupon tests. Coupons were machined from the complete sections of the wider-width regions (see Fig. 2) and subsequently tested in accordance with Code (GB/T 228- 2002). The key results of the coupon tests are summarised in Table 2.

Three different grades of commercial concrete strengths – C30, C40, and C50 – were used in the test. Six cubes (100 mm) of each batch were cast for material testing (GB 50152-92 1992), and the concrete elastic modulus and the average cubic strength (f_{cu}) at the time of testing have been illustrated in Table 3.

2.3 Experimental set-up

All column tests were performed in a 5000 kN capacity testing machine (See, Fig. 4). Axial shortening of the specimens was captured by means of 2 linear variable displacement transducers (LVDTs) positioned between the end platens of the aforementioned testing machine. Bearing plates were employed at both ends of the specimens as shown in Fig. 4. Strain gauges were used to measure the axial longitudinal strains and horizontal transverse strains at different locations along the steel tubes. Vertical strain gauges 100 mm apart were affixed to two perpendicular faces (that is to say, the wide and narrow face) of each specimen from a start-point 100 mm from the topmost location-point of the specimen. The number and position of the horizontal transverse strain gauges

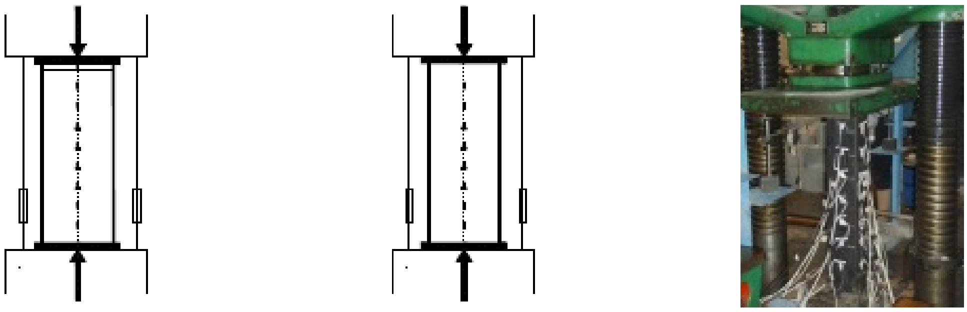

(a) Group ZYA (b) Group ZYB (c) Actual test

Fig. 4 Test set-up

was altered according to the various lengths of the specimens. The specific arrangement is as follows: for the columns of length 800 or 1000 mm, three horizontal strain gauges were affixed at the locations ($L/2-100$), $L/2$ and ($L/2+100$) mm, respectively; for the column with a length of 700 mm, two transverse strain gauges were affixed at the locations of ($L/2-50$) and ($L/2+50$) mm respectively; for the column with a longitude length of 900*mm*, four transverse strain gauges were affixed at the locations of ($L/2-150$), ($L/2-50$), ($L/2+50$) and ($L/2+150$) mm respectively. All transverse strain gauges were affixed to the wide face and narrow faces of the rectangular steel tubes.

A load interval of less than one tenth of the estimated strength was applied and all the specimens, except ZYA-3, were loaded continuously until point of failure. All tests were to be continued beyond the point of maximum load, with the period of unloading behaviour recorded dependant entirely on the practicability at the point of test arrangement. It should be noted that specimen ZYA-3 experienced two loading stages. When the load reached 650 kN, the test was stopped due to operational mistake. After the test machine was restarted, the load was reloaded until the specimen was destroyed. The progress of deformation, the mode of failure, and the maximum load taken by the specimens were duly recorded.

2.4 Experimental results and specimen behaviour

2.4.1 Failure mode

2.4.1.1 Steel loaded-first

As the load is applied on the steel tube in the first instance, the initial stiffness of each specimen is small and the strain on the steel tubes increased with the loading process. Once the load had reached the steel tube yield strength, the specimen showed axial compression and the deformation became more pronounced and the gap between the steel and the concrete at the loaded end became smaller gradually. At that moment, the loading increased slowly, and the loading method was changed to be full-section-loaded gradually. During the whole loading stage, some specimens showed symptoms of steel yield at the topmost location: where the gap is located. Then, with the axial deformation increasing at the same time, the load became heavier. When the load reached to its ultimate load, local buckling was found at certain positions near the two ends. This phenomenon usually occurred within the position of 1/3L – 1/4L away from the two ends of the specimens. The concrete around the local buckling positions crashed. After that the loading decreased gradually until the test stopped.

2.4.1.2 Full-section-loaded

At first, the deformation of the full section-loaded specimens (Group ZYB) showed a slight increase with the load. It's hard to find local buckling until the loads reached approximately the point of the ultimate load. After that, the development of the local buckling and the compressive deformation became obvious, and the axial deformation increased quickly.

2.4.1.3 Comparison between the two different loading methods

After the test, it can be seen all specimens showed at least one point of local buckling on each side, especially specimens with a larger cross section that showed two or three places of local buckling on each side. Each specimen only had one continuous buckling loop. The angle between the buckling loop and the horizontal plane was approximately 0-45°, and the buckling loop position appeared within the regions of 1/3L at the opposite top and bottom ends (see, Fig. 5).

The difference between the two loading methods is as follows: for the steel loaded-first method, some specimens with smaller cross-section show an obvious plastic deformation before or at the time of the two kinds of materials working together; meanwhile, for the full section loaded method, with the concrete and steel tube being subjected to the load simultaneously, the deformation change-rate was most rapid at a point in load just preceding the ultimate load. Besides, it should be noted that different damage positions may be owing to the cross-sectional property and the concrete curing quality. Meanwhile, some local buckling mainly occurred near the ends. This may be attributed to the fact that no end plates or stiffeners were used in the tests. The cross-section strength of the specimens may have not been achieved fully in this case.

2.4.2 Load-end shortening responses

The current test stub columns generally exhibited ductile behaviour. The load-end shortening curves derived from rectangular CFST columns axial compression tests are shown in Fig. 6. Comparing the relative specimens in Group ZYB with those of the full-section-loaded method, specimens in Group ZYA subjected to the steel-load exhibited lower yield strength, higher ultimate

(a) ZYA-6 (b) ZYA-5 (c) ZYB-7 (d) ZYB-9

Fig. 5 A view of specimen failure mode

strength and larger axial compression deformation. It can be found that all the Group ZYA specimens experienced two separate load ascending stages as recorded on the load-end shortening curves, with the exception of specimen ZYA-3 (due to the operational mistake, the recorded load-end shortening curve for specimen ZYA-3's behaviour reflects only the second load-stage).

To compare the final ultimate strength of specimens with the same geometry and material properties yet with different loading methods, a coefficient factor k, which is determined by N_{zya}/N_{zyb}, is proposed. Where N_{zya} is the ultimate strength of specimens with steel load, N_{zyb} is the ultimate strength of specimens with full-section load. k represents the enhanced value of different loading methods in relation to the ultimate carrying capacity. The value of k is listed in

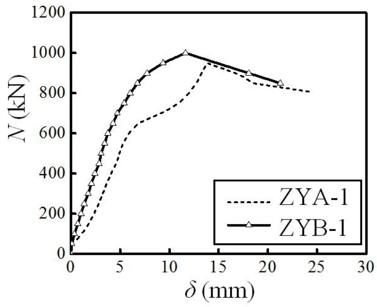

(a) ZY 1

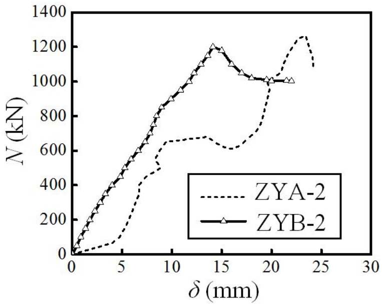

(b) ZY 2

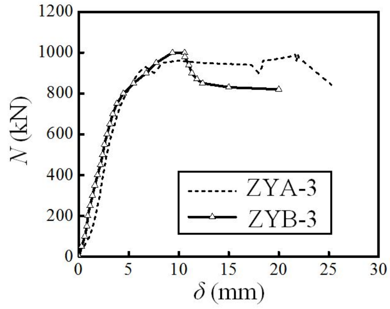

(c) ZY 3

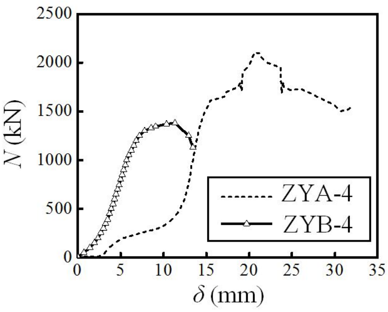

(d) ZY 4

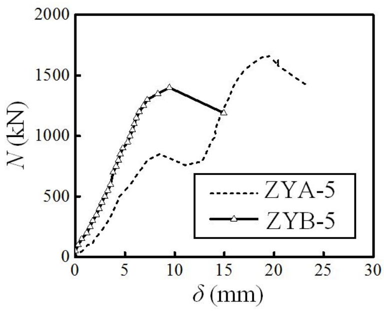

(e) ZY 5

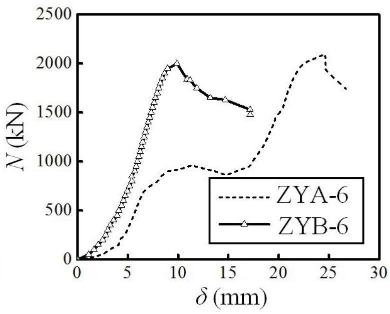

(f) ZY 6

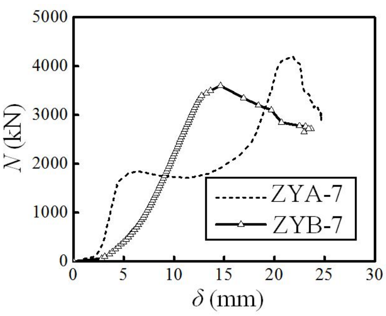

(g) ZY 7

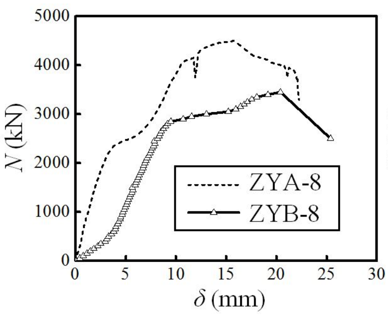

(h) ZY 8

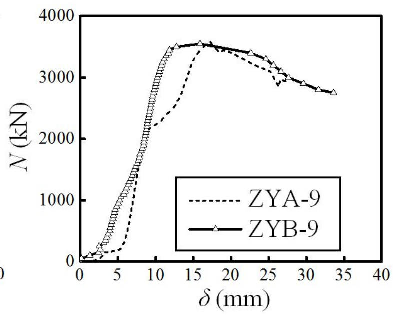

(i) ZY 9

Fig. 6 Load versus end shortening curves for each specimen

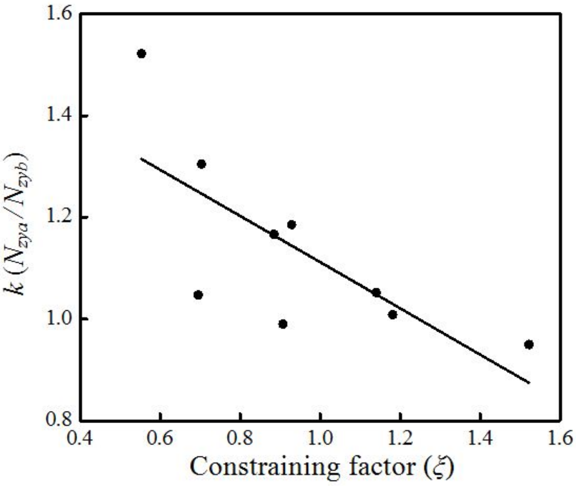

Fig. 7 ξ versus k relationship

Table 4 Comparisons between predicted column strengths and test results

Specimen number	N'_a	N_{zya}	N_{zyb}	SI		DI		$N_{a,pre}$	N_{GJB}	N_{EC4}	N_{ACI}	$N_{360\text{-}05}$	N_{LRFD}	k
				ZYA	ZYB	ZYA	ZYB							
1	650	950	1000	1.12	1.17	1.32	1.83	638	927	903	855	629	713	0.95
2	650	1262	1200	1.34	1.27	1.03	1.27	638	1046	1012	947	691	784	1.05
3	800	990	1000	0.96	0.96	1.04	1.17	638	1170	1123	1042	754	855	0.99
4	1500	2100	1380	1.25	0.82	1.13	1.17	806	1940	1856	1688	1254	1422	1.52
5	800	1660	1400	1.28	1.08	1.2	1.58	806	1438	1402	1302	967	1096	1.19
6	960	2095	2000	1.41	1.35	1.07	1.27	806	1685	1627	1493	1103	1251	1.05
7	1850	4200	3600	1.24	1.06	1.04	1.36	2068	3808	3682	3412	2539	2879	1.17
8	2350	4500	3450	1.19	0.91	1.39	1.13	2068	4313	4144	3805	2826	3204	1.30
9	1950	3580	3550	1.19	1.18	1.48	1.73	2068	3320	3230	3027	2246	2547	1.01

Table 4 and the relationship between k and ξ is shown in Fig. 7. It can be found that k decreases with the increase in ξ. The range of k is a figure between 0.95 and 1.52. This may be because steel tubes of Group ZYA resisted all the loads at first and showed local buckling at the early stage; this is due to the fact that the constraining force from the steel to the concrete core is smaller relative to the specimens subject to the full-section load. However, as more force is applied to the steel, the steel tube experienced a period of axial stress stiffening.

Furthermore, the results indicate that the measured elastic axial compressive stiffness alters as the load took changes. Comparing behaviours of the various specimens with the steel grade of Q345b (specimens ZYA7-9 and ZYB7-9), it can be found that the elastic axial compressive stiffness of these specimens subject to the steel-loaded method is greater, while, for specimens with the steel grade of Q235b (specimens ZYA1-6 and ZYB1-6), the elastic axial compressive stiffness of specimens with a full section-load is greater. Subsequent to the elastic compression stage, the axial compressive stiffness declined in a gradual way prior to the point of the final load being reached, but the total changes are still, altogether, small.

3. Analysis on test results and discussions

3.1 Poisson's Ratio

Poisson's Ratio is the ratio of the relative contraction strain, or transverse strain normal relative to the applied load, to the relative extension strain, or axial strain in the direction of the applied load. For the composite column, the Poisson's Ratio can be thought of as the absolute value of the steel outface transverse strain divided by the steel outface longitudinal strain (Schneider 1998). It can be expressed as

$$\upsilon = \varepsilon_t / \varepsilon_l \tag{2}$$

where υ is the Poisson's Ratio; ε_t is the transverse strain of steel tube; ε_l is the longitudinal strain of the steel tube.

The constraining behaviour imposed by the steel tube on the core concrete is a key feature of the rectangular CFST specimens. Due to this particular constraining force, the strength of the CFST columns was improved and turned out bigger than the sum of the strength of the steel and concrete in fact. The development of Poisson's Ratio represents the development of plastic deformation. The relationship between Poisson's Ratio and force can be used in the nonlinear analyses of deformation. Fig. 8 shows a comparison of the Poisson's Ratio to the axial load ratio (N/N_u) as applied to the specimens. Due to instrumental error and strain gauge vitiation, the Poisson's Ratio value in this particular graph constitutes the calculated values of longitudinal strain to transverse strain ratio at selected positions for each specimen. The legend displayed in the graph shows the selected position for each specimen. The symbols *N* and *W* represent the narrow face and wide face respectively and the figures after that represent the longitude from the loaded end.

It can be found the Poisson's Ratio does not linearly ascend with the axial load ratio at the early loading period, especially for Group ZYA specimens. Although the Poisson's Ratio of some specimens in Group ZYA increased abruptly at first, most of them were concentrated at the point of 0.3 at the load beginning. That may be because the load was applied on the steel first, and the bond strength between the steel and concrete core is very small (usually between 0.2 MPa and 0.4 MPa) for rectangular CFST members; therefore, the measured value is basically equal to the Poisson's Ratio of the steel. When loads near to 0.4 N_u, the Poisson's Ratio changes significantly. But for the specimen subject to the full section load, the values of Poisson's Ratio are concentrated between 0.2 and 0.3 at the outset. When loads near to 0.8 N_u, the Poisson's Ratio rose quickly in line with the rapid increase of the transverse strains.

3.2 Strength Index

The behaviour of concrete-filled tubes is clearly dependent upon a number of individual geometric and material parameters. The strength index (SI), which is adopted to quantify section strength, was applied herein to investigate the strength index of the tested specimens (Han 2002). The SI value reflects the contribution of positive interaction between the steel tube and the concrete infill for the column strength increment. It is defined as

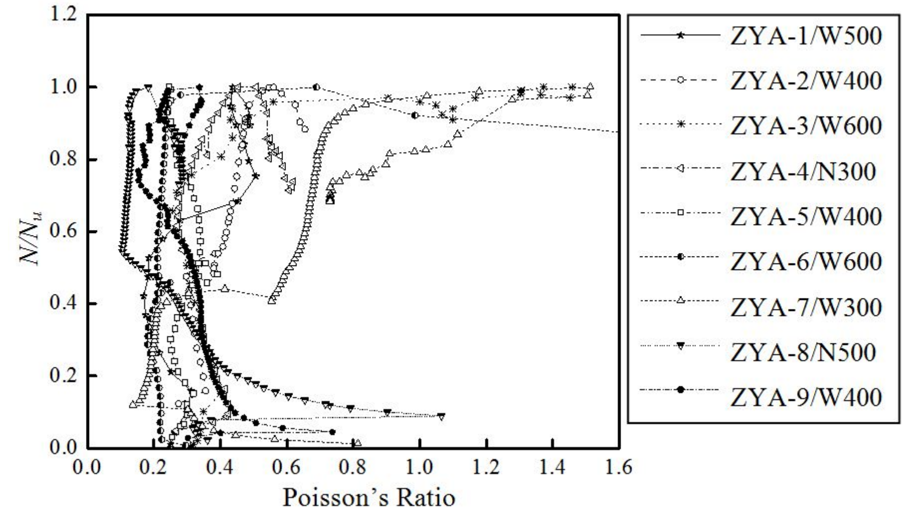

(a) Group ZYA

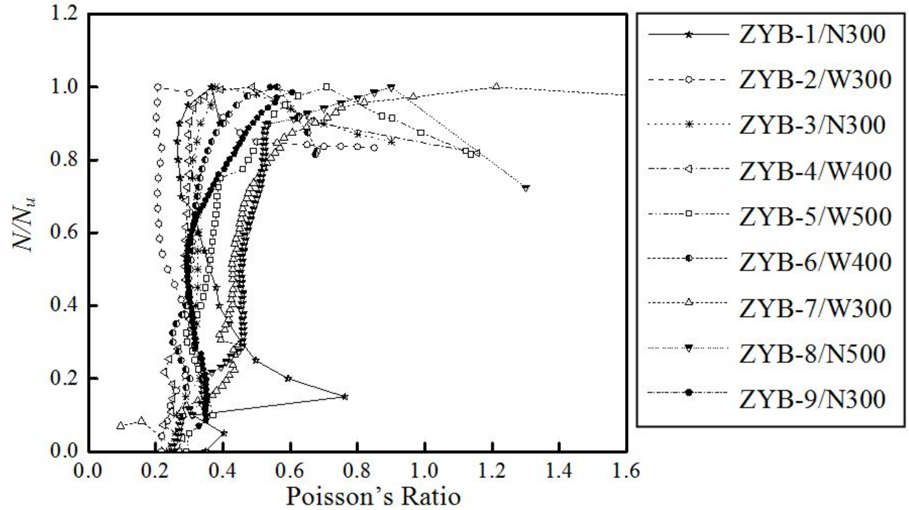

(b) Group ZYB

Fig. 8 Axial load ratio with respect to Poisson's Ratio

$$\mathrm{SI} = \frac{N_{u,e}}{A_s f_y + A_c f_{ck}} \tag{3}$$

The relationships between the ξ and SI of the test specimens are plotted in Fig. 9. It can be found that the variation tendency between ξ and SI are different for each loading method. For the full section-loaded specimens, the strength index increases with the increase of ξ, and this indicates that a stronger interaction exists for higher values of ξ. This accords with the conclusions obtained in past literature (Han 2002). However, for the steel-loaded method specimens (Group

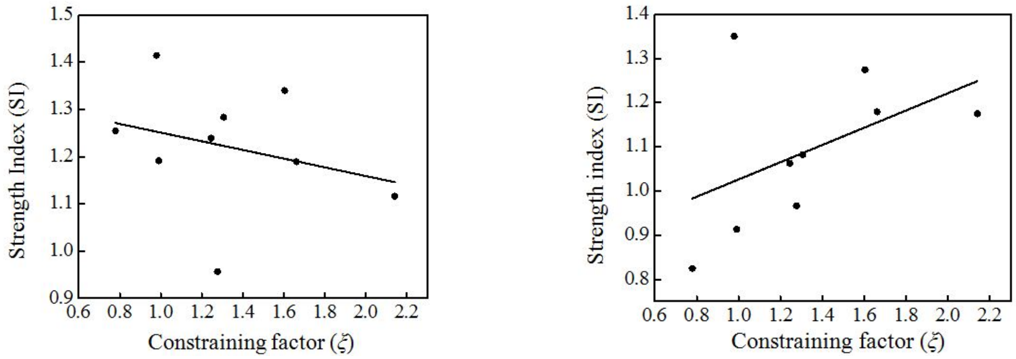

(a) Group ZYA (b) Group ZYB

Fig. 9 SI versus ξ relationship

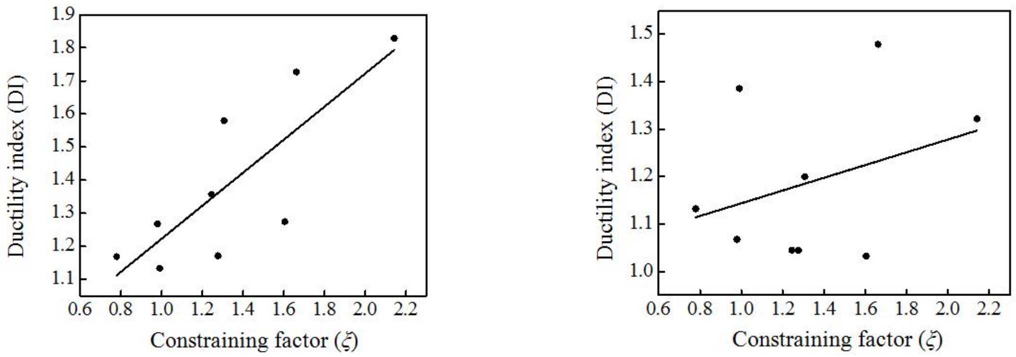

(a) Group ZYA (b) Group ZYB

Fig. 10 DI versus ξ relationship

ZYA), a negative, approximately linear trend emerges from the test data. It may be that more experiments are still needed to enlarge the scope of ξ to investigate the relationship between the two parameters to confirm these results. But it should be noted that, with the steel loaded-first method, most of the load's weight was transferred to the steel tubes at first and the steel was to experience sufficient axial compression. The steel stresses for some locations exceeded the yield strength. When the concrete and steel resisted loads concurrently the confining force which steel tube can offer to the concrete core decreased.

3.3 Ductility Index

One of the methods used to quantify section ductility is the ductility index. Several definitions of ductility index (DI) were used by various researchers based on load versus axial deformation curves or load versus axial strain curves. The ductility capacity of specimens in this study are based on the criterion applied in literature (Han 2002), DI = $\delta_{85\%} / \delta_u$(4), where δ_u is the axial deformation at the ultimate strength and $\delta_{85\%}$ is the axial deformation corresponding to the 85% of the ultimate strength of CFT columns measured after the ultimate strength has been reached.

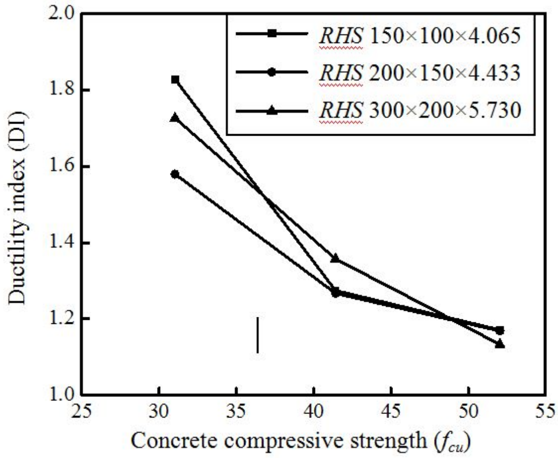

Fig. 11 DI versus f_{cu} relationship

The ductility indexes (DI) values so determined are presented in Table 1. Fig. 10 shows the influences of the constraining factor ξ on DI. It can be seen that, DI increases with the increase of the constraining factor. Comparing the value of the DI for the two groups, it can be found the loading method influences the DI value. Apart from specimens ZYA-3 and ZYB-3, the DI of other specimens that are fully section-loaded is slightly higher than those of the specimens that are steel-loaded. It indicates that the confinement received from the steel is slightly smaller for the steel loaded-first method specimens. The different result of the relative value of ZYA-3 and ZYB-3 may be due to the operational mistake and the selected test data for ZYA-3 is from the second loading stage. Moreover, Fig. 11 indicates the DI of Group ZYB is increased with the decrease of concrete strength grade. This may be due to the plastic deformation of concrete usually decreasing in extent concurrent with the increase of the concrete grade.

4. Analyses of test results and discussions

4.1 Distribution of axial load

There are three views on the calculation of axial pressure distribution coefficients for the steel tube and core concrete. One is based on the concept of the load being shared according to the material strength; the second is based on the load being shared by concrete as a priority. The third one is based on the Coordinated Deformation Theory. According to the second view, the load shared by the concrete took precedence: and when the load exceeds the concrete-carrying capacity, the left-over excess of the load is then shared by the steel tube. Therefore, the deformation effected in the CFST columns is explained in these terms: the steel tube has a smaller axial deformation, while the concrete core has a bigger axial deformation. This is not in agreement with the actual condition as is apparent. The calculated N_s / N, according to the Strength Theory and the Coordinated Deformation Theory for the tested specimens, are 0.35-0.59 and 0.46-0.64 respectively.

Due to the material properties of loading period. According to reference (Schneider 1998), the

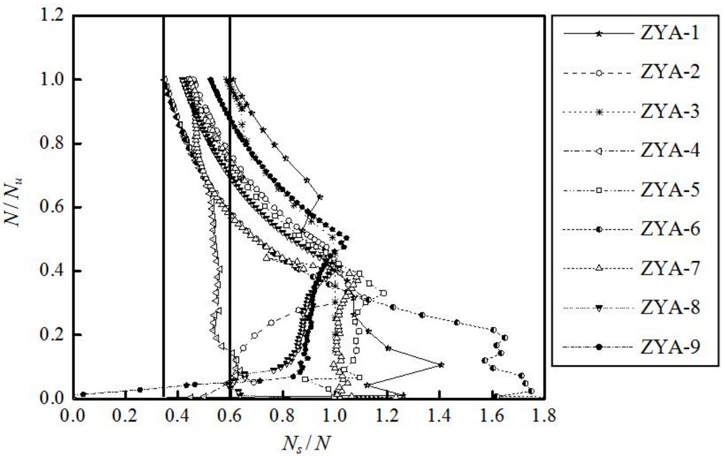

(a) Group ZYA

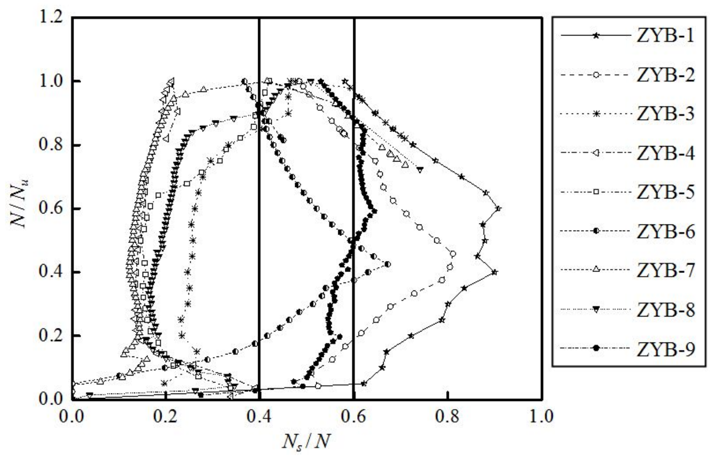

(b) Group ZYB

Fig. 12 Axial-to-ultimate load compared to load shared by the steel tube

load shared by the steel tube N_s was computed by averaging the values of the longitudinal strain gauges multiplied by the measured elastic modulus of the steel tube. Elastic, perfectly plastic strength was assumed for the steel tube once the yield steel and concrete, it is hard to monitor the actual distribution of the axial load during the whole l strain was exceeded. Fig. 12 illustrates the proportion of the total load shared by the steel section.

Group ZYA specimens showed an irregular increase in the total shared by the steel tube as the load approximately approached 0.4 N_u. After that the tendency between N_s/N and N/N_u decreased gradually. When the load reached to the ultimate load, the value of N_s/N stabilized between 0.4 and 0.6. While for Group ZYB specimens, the tendency between N_s/N and N/Nu is irregular across the whole loading period. However, when the load reached the point of ultimate load, the value of N_s/N of all this group's specimens stabilized between 0.35 and 0.55, except for specimen ZYB-4.

4.2 Discussion on the carrying capacity of test specimens

4.2.1 Steel loaded-first

It can be found from Fig. 6 that the ultimate strength of specimens subject to the steel loaded-first is higher than the relative steel tubes carrying capacity. Although the ultimate carrying capacity of specimens subjected to the steel-loaded method increased after the first yield, the deformation is too big when the load reaches to the ultimate strength, and the final damage suddenly occurred after the load reached to its ultimate strength. Therefore, the specimen yield resistance is more important than its ultimate strength for engineering design. Fig. 13 shows the relationship between the k' and the ξ, where $k' = N_{a'} / f_y A_s$ ($N_{a'}$ is the test yield resistance of Group ZYA). It can be found that k' decreased in line with the ξ. According to this, the predicted yield strength can be given as

$$N_{a,pre} = k' f_y A_s \tag{5}$$

where k' is the enhanced coefficient for the carrying capacity. It represents the contribution of the concrete infill to improving the steel tube resistance in its capacity to reduce the local buckling effect. According to the current test result it can be given at 1.1.

4.2.2 Full section-loaded

The section capacities predicted using five design methods (AISC 360-05 2005, LRFD 1999, BS EN 1994-1-1:2004 2009, ACI 318M-05 2005, GJB 4142-2000 2001) are compared with the stub column test results obtained in the current tests, supplemented by other experimental data from other literatures (Han 2002, Han and Yao 2003, Lue *et al*. 2007, Muhammad *et al*. 2006, Schneider 1998, Tao *et al*. 2009). Fig. 14 shows the comparison between design codes' predicted values and test data.

It can be concluded that EC4 (BS EN 1994-1-1 2009) and GJB (GJB 4142-2000 2001) expressions for rectangular CFST columns give closer predictions of the test results than others. The main reason for this conclusion is that GJB 4142-2000 (2001) expressions are proposed based

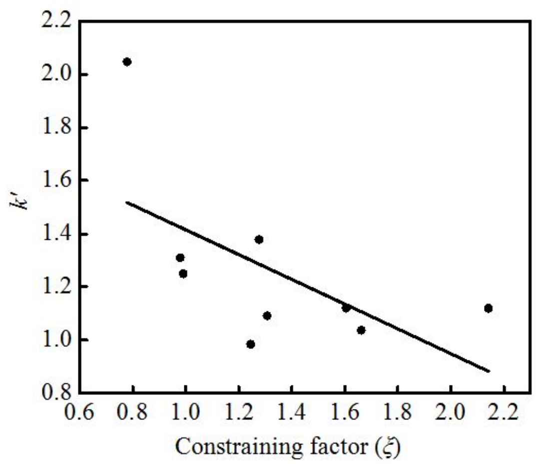

Fig. 13 k' versus ξ relationship

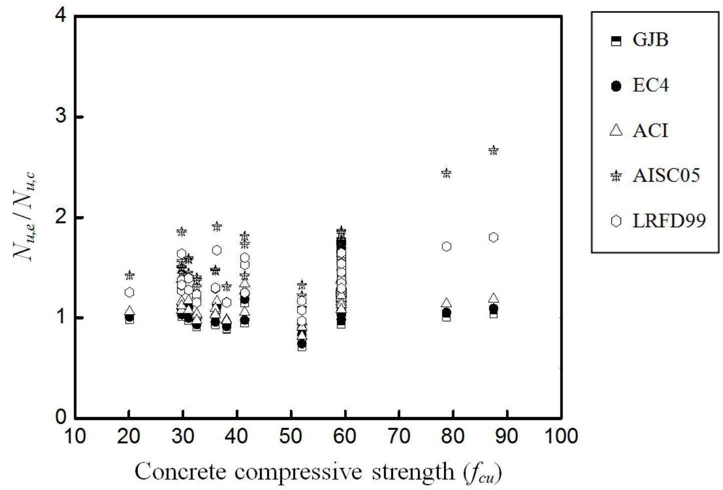

Fig. 14 Comparison of different design codes' calculated values

on a huge collection of experiment results. And the adopted material and property test measure methods are both typical in China and therefore there is a closer familiarity with this test. Therefore the result of the experiment conforms to the GJB expression. Based on the analysis of the axial load distribution and conclusions obtained from previous experimental studies on bond strength of rectangular CFST columns, the interface bond strength between the concrete and steel is very small. Therefore, the Superposition Theory is the most clear and appropriate theory available for the purpose of predicting the axial ultimate strength of rectangular CFST columns. As both the ACI (ACI 318M-05 2005) and AISC (AISC 360-05 2005) expressions adopt a 15% reduction of concrete strength on account of design safety degree, their prediction of ultimate carrying capacity is as such relatively conservative.

5. Conclusions

CFST columns are gaining increasing usage in modern construction practice with greater emphasis now being placed on durability and life-cycle costing. This paper focuses on the response of concrete filled rectangular steel tubular sections with different loading methods. A total of 18 stub columns were tested, nine being steel-loaded and nine full section loaded, and possessing varying steel strength grades, steel tube geometric properties and infill concrete strengths. The results, together with the supporting material and geometrical properties, have been reported. The development of Poisson's Ratio of specimens has been investigated. The strength and ductility indices' relationship with the constraining factor was studied. For the section-loaded specimens, the strength index increases with the increase of ξ, while for the steel-loaded-first method specimens a negative, approximately linear trend, emerges from the data. Meanwhile the ductility index of the two groups increases with the increase in the constraining factor. Moreover, the DI of specimens subjected to full section-loading increases with the decrease in concrete strength grade. Comparing the ultimate strength of the two groups, the final strength of Group ZYA is slightly greater than that of Group ZYB and the ratio value of k (N_{zya}/N_{zyb}) decreases with the increase in ξ.

A predicted expression has been proposed to calculate the ultimate strength for specimens with steel-loaded-first method applied at one end. For the full section-loaded method, comparisons of attained capacities from the tests presented herein, together with comparisons of other available results from the relevant literature, have been performed with existing design models of composite carbon steel sections – EC4, ACI 318M-05 (2005), AISC 360-05 (2005), GJB 4142-2000 (2001) and AISC 360-05 (2005) / LRFD (1999). The conclusion is that EC4 and GJB expressions for rectangular CFST columns give closer predictions of the test results than others. This investigation has focused on the axial cross-section capacity; and further experimental and analytical research is required to verify the applicability of the approaches at member level.

Acknowledgments

This paper is supported by the National Natural Scientific Fund-Youth Science Fund Project "Research on Cooperativity and Composite Mechanical Performance for High-Performance Rectangular Concrete-filled Steel Tubular Columns" (51408026). The authors are also grateful to the China Standard Management Group for the GB50017-2003 Structural Steel Design Code for their special composite structure research funding (GB 5000172010-04), and would like to thank the Taian Kenuo profile steel stock company limited for the supply of test specimens and Butler (Tianjin) Inc., for their help with this project and research students in the steel research group of Tianjin University for their assistance with the laboratory work.

References

ACI 318M-05 (2005), Building code requirements for structural concrete and commentary, ACI Committee 318.

AISC 360-05 (2005), Specification for structural steel buildings, AISC, Chicago, IL, USA.

BS EN 1994-1-1:2004 (2009), Eurocode 4: Design of composite steel and concrete structures – part1-1: General rules for buildings, London, UK.

Chen, B.C. and Huang, F.Y. (2009), "Experimental research on influence of loading methods to behavior of concrete filled steel tubular stub columns under axial loads", *J. China Railway Soc.*, **31**(3), 82-88. [In Chinese]

Dai, X.H. and Lam, D. (2012), "Shape effecton thebehaviourofaxially loaded concrete filled steel tubular stub columns at elevated temperature", *J. Construct. Steel Res.*, **73**, 117-127.

EI-Heweity, M.M. (2012), "On the performance of circular concrete-filled high strength steel columns under axial loading", *Alexandria Eng. J.*, **51**(2), 109-119.

Ellobody, E. (2007), "Nonlinear behaviour of concrete-filled stainless steel stiffened slender tube columns", *Thin-Wall. Struct.*, **45**(3), 259-273.

GB 50152-92 (1992), Standard methods for testing of concrete structures, Chinese Standard, Beijing, China. [In Chinese]

GB/T 228-2002 (2002), Metallic materials - Tensile testing at ambient temperature, Chinese Standard, Beijing, China. [In Chinese]

Giakoumelis, G. and Lam, D. (2004), "Axial capacity of circular concrete-filled tube columns", *J. Construct. Steel Res.*, **60**(7), 1049-1068.

GJB 4142-2000 (2001), Technical specifications for early-strength model composite structure used for navy port emergency repair in wartime, Chinese Standard, Beijing, China. [In Chinese]

Gupta, P.K., Sarda, S.M. and Kumar, M.S. (2007), “Experimental and computational study of concrete filled steel tubular columns under axial loads”, *J. Construct. Steel Res.*, **63**(2), 182-193.
Han, L.H. (2002), “Tests on stub columns of concrete-filled RHS sections”, *J. Construct. Steel Res.*, **58**(3), 353-372.
Han, L.H. and Yao, G.H. (2003), “Behaviour of concrete-filled hollow structural steel (HSS) columns pre-load on the steel tubes”, *J. Construct. Steel Res.*, **59**(12), 1455-1475.
Han, L.H., Zhao, X.L. and Tao, Z. (2001), “Tests and mechanics model for concrete-filled SHS stub columns, columns and beam-columns”, *Steel Compos. Struct.*, *Int. J.*, **1**(1), 51-74.
Lam, D., Dai, X.H. and Han, L.H. (2012), “Behaviour of inclined, tapered and STS square CFST stub columns subjected to axial load”, *Thin-Wall. Struct.*, **54**, 94-105.
Liang, Q.Q. (2011), “High strength circular concrete-filled steel tubular slender beam–columns, Part II: Fundamental behavior”, *J. Construct. Steel Res.*, **67**(2), 172-180.
Load and Resistance Factor Design (1999), Specification for Structural Steel Buildings: American Institute of Steel Construction, Chicago, IL, USA.
Lue, D.M., Liu, J.L. and Yen, T. (2007), “Experimental study on rectangular CFT columns with high-strength concrete”, *J. Construct. Steel Res.*, **63**(1), 37-44.
Moon, J., Roeder, C.W., Lehman, D.E. and Lee, H. (2012), “Analytical modeling of bending of circular concrete-filled steel tubes”, *Eng. Struct.*, **42**, 349-361.
Muhammad, N.B., Fan, J.S. and Nie, J.G. (2006), “Strength of concrete filled steel tubular columns”, *Tsinghua Sci. Tech.*, **11**(6), 657-666.
Patel, V.I., Liang, Q.Q. and Hadi, M.N.S. (2012), “High strength thin-walled rectangular concrete-filled steel tubular slender beam-columns, Part I: Modeling”, *J. Construct. Steel Res.*, **70**, 377-384.
Schneider, S. (1998), “Axially loaded concrete-filled steel tubes”, *J. Struct. Eng.*, **124**(10), 1125-1138.
Song, T.Y., Han, L.H. and Yu, H.X. (2010), “Concrete filled steel tube stub columns under combined temperature and loading”, *J. Construct. Steel Res.*, **66**(3), 369-384.
Tao, Z., Uy, B., Han, L.H. and Wang, Z.B. (2009), “Analysis and design of concrete-filled stiffened thin-walled steel tubular columns under axial compression”, *Thin-Wall. Struct.*, **47**(12), 1544-1556.
Tokgoz, S. and Dundar, C. (2010), “Experimental study on steel tubular columns in-filled with plain and steel fiber reinforced concrete”, *Thin-Wall. Struct.*, **48**(6), 414-422.
Xiong, D.X. and Zha, X.X. (2007), “A numerical investigation on the behaviour of concrete-filled steel tubular columns under initial stresses”, *J. Construct. Steel Res.*, **63**(5), 599-611.
Yang, Y.F. and Han, L.H. (2009), “Experiments on rectangular concrete-filled steel tubes loaded axially on a partially stressed cross-sectional area”, *J. Construct. Steel Res.*, **65**(8-9), 1617-1630.
Yang, H., Lam, D. and Gardner, L. (2008), “Testing and analysis of concrete-filled elliptical hollow sections”, *Eng. Struct.*, **30**(12), 3771-3781.
Yuan, W.B. and Yang, J.J. (2013), “Experimental and numerical studies of short concrete-filled double skin composite tube columns under axially compressive loads”, *J. Construct. Steel Res.*, **80**, 23-31.

CC

Symbols

A_c	Cross-sectional area of concrete core;
A_s	Cross-sectional area of steel tube
B	Width of the rectangular steel tube;
D	Depth of the rectangular steel tube;
DI	Ductility index;
E_c	Young's modulus of concrete;
E_s	Young's modulus of rectangular steel tube;
f_c'	Specified compressive strength of concrete;
f_{cu}	Compressive cube strength of concrete;
f_y	Yield strength of steel;
f_u	Ultimate strength of steel;
k	Ultmate strength of specimens with steel to ultimate strength of specimens with full section oaded ($N_{\mathrm{zya}} / N_{\mathrm{zyb}}$);
k'	Enhanced coefficient for the axial compression carrying capacity with steel loading method;
L	Length of the rectangular steel tube;
N_a'	Test yield resistance of Group ZYA;
$N_{a,pre}$	Predicted yield resistance of concrete-filled rectangular specimens with steel loaded method
N_{ACI}	Predicted resistance of concrete-filled rectangular specimens according to ACI318M-05;
N_{EC4}	Predicted resistance of concrete-filled rectangular specimens according to EC4;
N_{GJB}	Predicted resistance of concrete-filled rectangular specimens according to GJB 4142-2000 (2001);
N_{LRFD}	Predicted resistance of concrete-filled rectangular specimens according to AISC 360-05 (2005) / LRFD (1999);
N_u	Ultimate axial compression carrying capacity;
$N_{u,c}$	Predicted resistance of concrete-filled rectangular specimens according to design codes;
$N_{u,e}$	Ultimate test resistance of concrete-filled rectangular specimens;
$N_{360\text{-}05}$	Predicted resistance of concrete-filled rectangular specimens according to AISC 360-05 (2005);
SI	Strength index;
t	Wall thickness of the steel tube;
ξ	Constraining factor;
δ	Specimen end shortening;

$\delta_{85\%}$	Axial deformation corresponding to the 85% of the ultimate strength of CFST columns measured after the ultimate strength was reached;
δ_u	Axial deformation at the ultimate strength;
υ	Poisson's ratio;
ε_t	Transverse strain of steel tube;
ε_l	Longitudinal strain of steel tube.